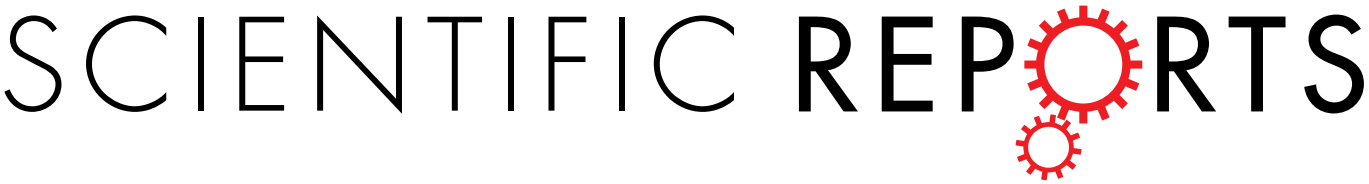

OPEN

Direct observation of photocarrier electron dynamics in C_{60} films on graphite by time-resolved two-photon photoemission

Received: 08 July 2016
Accepted: 06 October 2016
Published: 24 October 2016

Masahiro Shibuta[1], Kazuo Yamamoto[2], Tsutomu Ohta[2], Masato Nakaya[2,3], Toyoaki Eguchi[2,3] & Atsushi Nakajima[1,2,3]

Time-resolved two-photon photoemission (TR-2PPE) spectroscopy is employed to probe the electronic states of a C_{60} fullerene film formed on highly oriented pyrolytic graphite (HOPG), acting as a model two-dimensional (2D) material for multi-layered graphene. Owing to the in-plane sp^2-hybridized nature of the HOPG, the TR-2PPE spectra reveal the energetics and dynamics of photocarriers in the C_{60} film: after hot excitons are nascently formed in C_{60} via intramolecular excitation by a pump photon, they dissociate into photocarriers of free electrons and the corresponding holes, and the electrons are subsequently detected by a probe photon as photoelectrons. The decay rate of photocarriers from the C_{60} film into the HOPG is evaluated to be $1.31 \times 10^{12}\ s^{-1}$, suggesting a weak van der Waals interaction at the interface, where the photocarriers tentatively occupy the lowest unoccupied molecular orbital (LUMO) of C_{60}. The photocarrier electron dynamics following the hot exciton dissociation in the organic thin films has not been realized for any metallic substrates exhibiting strong interactions with the overlayer. Furthermore, the thickness dependence of the electron lifetime in the LUMO reveals that the electron hopping rate in C_{60} layers is $3.3 \pm 1.2 \times 10^{13}\ s^{-1}$.

Research on the two-dimensional (2D) graphene material, which consists of a sp^2 carbon network, has recently received a great deal of attention owing to its remarkable physical properties[1,2], such as high electron conductivity and chemical stability, as well as optical transparency. While many practical possible usages of graphene have been proposed, a combination of graphene and an organic molecular film is of particular interest[3–14], because they nicely suit the requirements for the next generation of low-cost, flexible, large area optical and electronic devices. From these viewpoints, an investigation of the electronic interaction and charge carrier dynamics at the graphene-organic interface is one of the key issues to resolve in the dawning era of graphene-based functional devices. Although the characteristics of organic molecules or functional nanomaterials deposited on a graphene surface have been investigated in this decade with scanning probe microscopy[4,6,8,9,12], there have been few spectroscopic investigations relevant to the electronic structures and carrier dynamics at the hetero surface and interface.

Fullerene C_{60}, consisting of a sp^2 carbon network, is one of the materials most studied as a functional organic semiconductor since its discovery[15] and it is also known to be a good electron acceptor for organic photovoltaic (OPV) devices, including solar cells, owing to its high electron affinity[16–21]. Indeed, graphene-C_{60} based OPV devices have been recently fabricated by several groups[3,7,11,14]. Since the transport gap (E_t) of crystalline C_{60} is believed to be 2.3–2.4 eV[22], it is likely that free photocarriers are generated with a photon energy ($h\nu$) considerably higher than 2.3–2.4 eV by the dissociation of highly-excited excitons (hot exciton). In fact, efficient photoconductance appears in a C_{60} film at $h\nu > 2.3$ eV[23]. So far, the ultrafast dynamics of photoexcited electronic states of C_{60} has been studied by several research groups[24–30], but there are still insufficient spectroscopic investigation tracking precisely the photocarrier electron generated in C_{60} thin films.

[1]Keio Institute of Pure and Applied Science (KiPAS), Keio University, 3-14-1 Hiyoshi, Kohoku-ku, Yokohama 223-8522, Japan. [2]Department of Chemistry, Faculty of Science and Technology, Keio University, 3-14-1 Hiyoshi, Kohoku-ku, Yokohama 223-8522, Japan. [3]JST, ERATO, Nakajima Designer Nanocluster Assembly Project, 3-2-1 Sakado, Takatsu-ku, Kawasaki, 213-0012, Japan. Correspondence and requests for materials should be addressed to A.N. (email: nakajima@chem.keio.ac.jp)

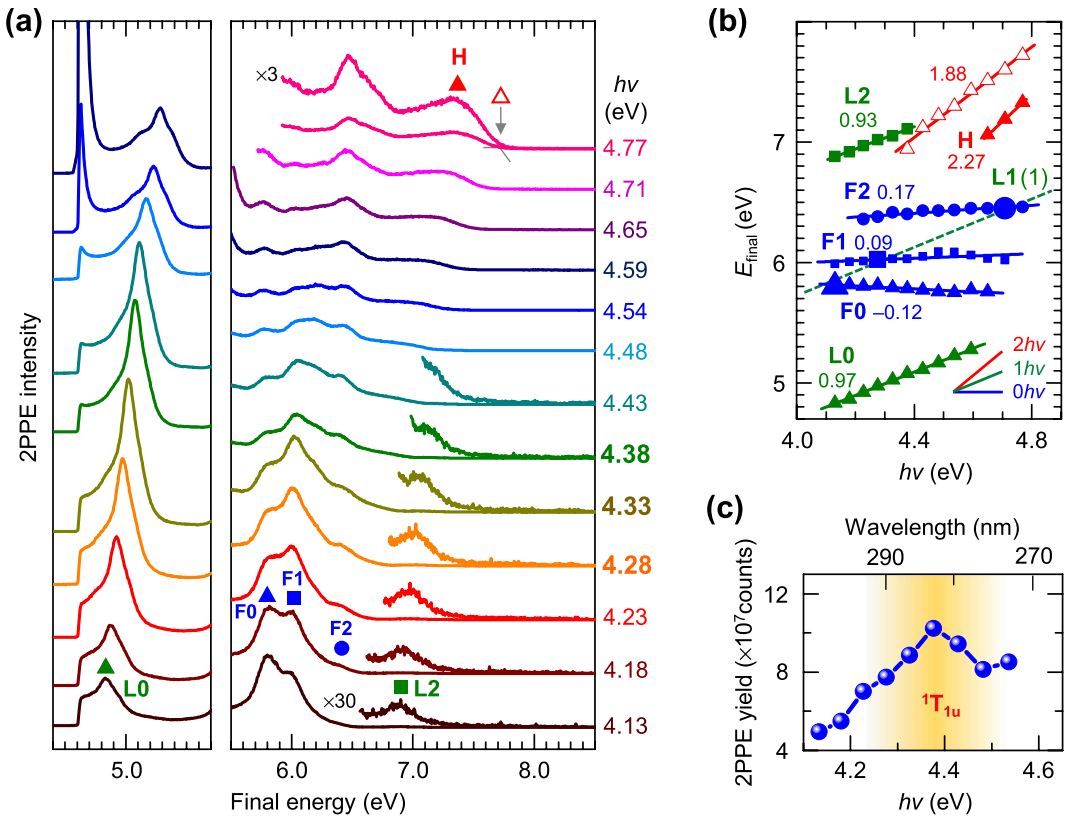

Figure 1. 2PPE of 1 ML C_{60} on HOPG. (**a**) $h\nu$ dependences of 2PPE spectra for 1 ML C_{60} film on HOPG aligned with E_{final}, where the $h\nu$ range was 4.13–4.77 eV. (**b**) Energy positions of 2PPE structures including the onset of H against $h\nu$, which are assignable to the slope of "0 $h\nu$", "1 $h\nu$", or "2 $h\nu$". Factors obtained by liner fits of the plots are indicated nearby the data. The dotted line shows the "1 $h\nu$" slope by an unoccupied level at $E_F + 1.8$ eV (see text). (**c**) Total 2PPE yield integrated whole energy region versus $h\nu$ in which the maximum is corresponding to that optical absorption ($^1T_{1u}$) of C_{60} film. Note that recovering intensity at the highest $h\nu$ is due to a contribution of one photon photoemission.

In this article, we present a spectroscopic study of photocarrier electron dynamics of C_{60} deposited on a highly-oriented pyrolytic graphite (HOPG) as a model for multi-layered graphene by means of time-resolved two-photon photoemission (TR-2PPE) spectroscopy. The TR-2PPE unveils the ultrafast dynamics of electronically excited states on a surface system with femtosecond (fs = 10^{-15} s) time resolution[31,32], and it has lately begun to be applied to graphene-related surfaces[33,34].

The experimental results reveal that the energy levels of C_{60}, which are independent of the C_{60} coverage, are little influenced by the 2D electronic nature of the in-plane sp^2 carbon network; the overlayer molecular C_{60} film is electronically decoupled from the HOPG substrate. The photoexcited electron behavior in the lowest unoccupied molecular orbital (LUMO) of C_{60} suggests that free photocarrier electrons are generated by the dissociation of hot excitons without forming lower-lying excitons. The decay rate of photocarrier electrons into the HOPG substrate is very low (1.31×10^{12} s^{-1}) compared with that on metallic substrates, which is also a characteristic of the 2D substrate. Moreover, thanks to the 2D nature of the material, it is revealed that the photocarrier electron hopping rate in C_{60} layers is $3.3 \pm 1.2 \times 10^{13}$ s^{-1}, from the C_{60} thickness dependence of the TR-2PPE measurements.

Results and Discussion

Energy levels of C_{60} monolayer on HOPG. Figure 1a shows 2PPE spectra for a C_{60} monolayer (1 ML, see Supplementary Figs S1 and S2 for the coverage calibration) formed on HOPG by changing the incident $h\nu$ at ~0.05 eV intervals. The photoelectrons emitted with surface normal ($k_{//} = 0$) were recorded with a limited acceptance angle of ± 0.6°. The horizontal axis shows the final state energy (E_{final}) relative to Fermi level (E_F). Six spectral features labeled as L0, L2, F0, F1, F2, and H appear by the formation of C_{60} film. The vacuum level (E_{vac}) is located at 4.60 eV above E_F obtained from the energy of the low energy cut-off of the spectra with lower photon energy, while the intensity around the cut-off becomes stronger at $h\nu \geq E_{vac}$ because of signals from direct (one-photon) photoemission. When the peak positions in the 2PPE spectra, including a threshold of H (red open triangle), are plotted in Fig. 1b versus $h\nu$, they can be assigned to an initial, intermediate, or final state[35]; an occupied state below E_F (initial state: $E = E_{final} - 2\ h\nu$), an unoccupied state between E_F and E_{vac} (intermediate state: $E = E_{final} - 1\ h\nu$), or an unoccupied state above E_{vac} (final state: $E = E_{final}$) are distinguished, whose shifts are proportional to 2 $h\nu$, 1 $h\nu$, and 0 $h\nu$, respectively. Note that the intensities of final states are enhanced at specific $h\nu$ marked by larger symbols in Fig. 1b owing to a resonance with an intermediate unoccupied state at $E_F + 1.8$ eV, labeled by L1. In

fact, the larger symbols are consistently fitted by a slope of 1 $h\nu$ as a dotted line superimposed in Fig. 1b. Note that, the L1 structure appears more clearly in the 2PPE spectra with a wider acceptance angle (Supplementary Fig. S1) or in angle-resolved 2PPE (Supplementary Fig. S3), because it has an electronic resonance with dispersive F0–F2, as discussed below. Including the state at $E_F + 1.8$ eV, the 2PPE spectra unveil seven electronic states; one occupied state located at $E_F - 2.2$ eV (H), three unoccupied states between E_F and E_{vac} at E_F +0.7 (L0), +1.8 (L1), and +2.7 eV (L2), and three unoccupied states above E_{vac} at E_F +5.8 (F0), +6.0 (F1), and +6.5 eV (F2). Although the peak H (red solid triangle) is broadened below $h\nu = 4.6$ eV, which is assignable to an occupied state, judging from the plot of the slope aligning with 2 $h\nu$, including that of higher energy thresholds (red open triangle).

The series of F0–F2 states show large band dispersions parallel to the surface from an angle-resolved 2PPE measurement, while the others have little dispersion (see Supplementary Fig. S3). The result suggests that F0–F2 are assignable to a series of higher-lying superatomic molecular orbitals (SAMOs)[36–41]; the wavefunctions of SAMOs generally diffuse outside the molecular framework, which would form highly dispersive band structures in a molecular film with a periodic surface structure. As shown in Fig. 1a, F0–F2 are enhanced only around non-dispersive L1 (Supplementary Fig. S3), suggesting that the observation of SAMOs in 2PPE requires an initial or intermediate electronic state to allow the resonance. It is known that the lowest (1s-) SAMO is experimentally observed at around $E_F + 3.3$–3.8 eV in a C_{60} monolayer on noble metal substrates with a strongly delocalized nature[36,38–40]. The absence of the 1s-SAMO in our study is attributable to the 2D electronic structure of the HOPG substrate; since the electronic structures of graphene below and above E_F are governed by sp^2 hybridized orbitals oriented parallel to the graphene plane, the chemical interaction with the overlayer material is very weak compared to metallic materials[8]. In fact, the energetics of a C_{60} film are almost independent (± 0.1 eV) of the C_{60} coverage from 1 to 30 ML (see Supplementary Fig. S4), while metallic substrates considerably perturb the electronic states of C_{60}, especially for the first layer, by strong metal-molecule coupling at the interface. Owing to the weak chemical interaction, an electron excitation through the conduction band of the substrate into the unoccupied states of C_{60} film would be unlikely. For C_{60} on HOPG, electron excitation into the 1s-SAMO is allowed only from an occupied level (e.g. the highest occupied molecular orbital (HOMO)) of C_{60} with intra- or inter-molecular excitation. Since the onset of the HOMO is E_F–1.8 eV from the ultraviolet photoelectron spectroscopy (UPS) (Supplementary Fig. S5), the HOMO electron cannot access energetically to the 1s-SAMO with the current $h\nu$s (4 – 5 eV). Indeed, the 1s-SAMO observed in a 1 ML C_{60} film on Ag(111) with a similar $h\nu$ quickly disappeared on additional C_{60} deposition[38], indicating that injection of electrons from a metal substrate is essential to resolve the 1s-SAMO with the $h\nu$ range used here.

More importantly, we now focus on the observed energy levels of H and L0–L2, which are essential to understand the electronic and optical properties of the C_{60}-HOPG system, rather than higher-lying C_{60} SAMOs. Comparing with UPS result (see Supplementary Fig. S5), the peak H is assignable to HOMO of C_{60}[22,42].

For the assignments of L0, Dutton *et al.* had initially assigned it to LUMO of C_{60}[28], where they observed very similar 2PPE spectra with the present result for >2 ML C_{60} coverages of Cu(111) substrate. However, they subsequently reassigned the corresponding peak (L0) to the next LUMO (LUMO + 1) involved in Frenkel excitions[29,43]. The main reason of their change in the assignment relied on the energy matching with a theoretical result for the optical transition in solid C_{60}[44]. They have also argued that the LUMO (exciton) is expected to be located at slightly above E_F, which cannot be resolved using their experimental conditions. Another 2PPE group using a pump photon of 3 eV has insisted on other assignments of 2PPE structures; peaks observed at HOMO + 2.2 eV, and +3 eV are attributed to free photocarrier electron in LUMO, and LUMO + 1, respectively[26,27]. In spite of their previous (re)assignments, judging from our experimental findings on HOPG substrate, it should be more reasonable to assign L0 located at HOMO + 2.9 eV as a photocarrier electron in LUMO for the following reasons.

C_{60} has a HOMO (h_u) and LUMO (t_{1u}), with an optical gap (E_{opt}) of 1.7–1.9 eV[45–47]. The UPS and inverse photoemission spectroscopy (IPES) for a C_{60} film have shown that the LUMO is observed at $E_F + 0.6$ eV, which provides the HOMO-LUMO gap (ΔE) of 2.35 eV[48]. The energy difference ($\Delta E - E_{opt}$) is attributed to on-site Coulomb energy (exciton binding energy), U.

In the 2PPE spectroscopy, occupied states in a cationic final state are probed similar to UPS, whereas unoccupied states reflect a neutral or cationic final state depending on the excitation processes. There are two photoemission pathways via an unoccupied state: (1) When electrons are supplied from a donor state with a pump photon, the molecule can be regarded as an anion, and then the electron occupying originally unoccupied states is emitted by a probe photon. A probe photon of 2−6 eV can emit the photoelectron mainly from molecular anions in the top layer owing to the limited escape depth of electrons. In fact, the 2PPE spectra for 1 ML C_{60}/Au(111), which show a strong molecule-substrate interaction are markedly changed at 2 ML[29], suggesting that the photoelectron escape depth is around or smaller than the thickness of one monolayer.

The other pathway of (2) is via an intra-molecular excitation, in which a photo-excited *e-h* pair is localized at a molecule, resulting in a larger excitonic interaction between the electron and hole. After the intra-molecular excitation, the electron is emitted with the probe photon, where there are two channels of photoelectrons (2a) from the exciton and (2b) from photocarrier electrons. The latter is generated by the hot exciton dissociation into a free electron and hole.

For the C_{60} in the outermost layer, furthermore, the number of surrounding C_{60} molecules is smaller than that inside the C_{60}, and then the polarization energy to stabilize a charged molecule becomes smaller for the surface molecules. In other words, the less crowded surroundings result in the increase of U, and the ΔE of the outermost layer is larger than that in the bulk. This effect should be paid attention to when the values are compared among the results of UPS, IPES, and 2PPE spectroscopy.

In bulk C_{60}, ΔE has been estimated to be 2.35 eV from the thresholds of UPS and IPES[49], while ΔE is 2.9 eV in the 2PPE spectroscopy obtained from H and L0 peaks. Based on the assignment of L0, indeed, the successive L1 and L2 peaks are assignable to LUMO + 1 and LUMO + 2 with reasonable energy positions observed by IPES[22,42].

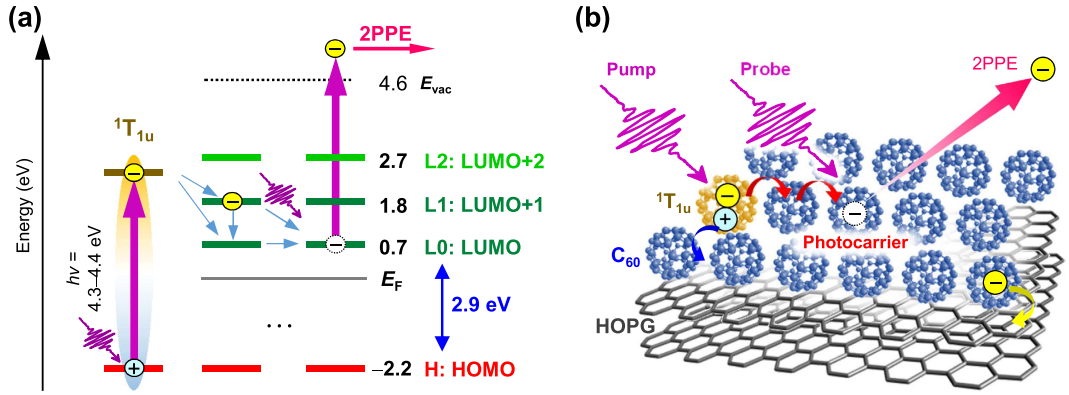

Figure 2. Energy diagram of observed energy levels. (**a**) Energy diagram of occupied and unoccupied levels near E_F as well as a hot exciton state of $^1T_{1u}$. F0–F2 located above E_{vac} are not addressed in (**a**,**b**) Drawing of the hot exciton dissociation and hopping processes during the 2PPE.

These consistent results show that L0 is assignable to the LUMO of a neutral C_{60}, where the photoemission from L0 occurs via process (2b).

It is known that ΔE for a C_{60} monolayer on a metal substrate is small compared to that in the bulk C_{60}, because the on-site charge is more effectively screened by the substrate than by a C_{60} film, resulting in a reduction of U[49–51]. As mentioned above, the energy positions are almost identical regardless of the C_{60} coverage on HOPG (Supplementary Figs S1 and S4), which shows that the screening effect from HOPG is much smaller than that from a metal substrate, due to its low density of states near E_F. Furthermore, as discussed below, electrons in L0 have a long lifetime of several picoseconds, also indicating that L0 *does not* originate from the LUMO + 1 involved in Frenkel excitions, as pervious reassignments[29,43], otherwise it would decay rapidly into lower-lying states within a few hundred fs[52–54]. Another 2PPE group has observed a peak at HOMO + 2.2 eV using a 3 eV pump photon, and they have assigned it to the free photocarrier electron in the LUMO[26,27]. However, we believe the assignment is not appropriate, because the peak to peak energy separation of 2.2 eV is too small to assign to a free photocarrier in the LUMO, considering that the ΔE of 2.3 eV defined by the respective onset edges in the UPS and IPES spectra.

Despite the above, it seems reasonable that hot excitons are generated by pump photon in 2PPE spectroscopy. Figure 1c shows the $h\nu$ dependence of the total 2PPE yield, which reaches a maximum at $h\nu = 4.3$–4.4 eV, implying a resonant photo-excitation in the C_{60} film. This energy indeed corresponds to the optical absorption of a C_{60} film (280 nm in wavelength)[23,55], assignable to the third optically allowed resonance of 3^1T_{1u}[56] marked in Fig. 1c. As seen in Fig. 1a, the intensity of LUMO + 2 at $E_F + 2.7$ eV is much weaker than that of the LUMO and LUMO + 1, also implying that electrons are dominantly excited from the HOMO at $E_F - 2.2$ eV with current $h\nu$ of 4.8 eV at most; while the contribution of occupied states in HOPG is rather small. Therefore, it can be considered that hot excitons are nascently generated in the C_{60} film by a pump photon and subsequently dissociate into a free electron and hole without relaxing into lower-lying excitons. The excited electron temporally occupies LUMOs of surrounding non-excited C_{60}, and is finally detected as a photoelectron excited by a probe photon. One may wonder why the hot exciton (3^1T_{1u}) is not resolved as an individual peak in the 2PPE spectra. The absence of the initially-excited hot exciton in 2PPE spectra would imply a very fast (<sub 10 fs) process of hot exciton dissociation, which broadens the spectral feature of the excitonic state (lifetime broadening)[32]. The observed energy levels and the excitation and detection scheme in 2PPE process are schematically illustrated in Fig. 2a,b. Here, it is not exclusive for a charge transfer (CT) state of $C_{60}^+C_{60}^-$ to be involved, and the CT state is actually predicted to be located at HOMO + 2.3 eV in theoretical calculations[57]. Formation of the lowest-lying excitons such as S_1 and T_1 would be another pathway of hot electron relaxation that may induce the photoemission by process 2a described above. The central energy of S_1 (0-0 transition) is known to be 2.0 eV, whereas the absorption band of S_1 distributes from 430 to 670 nm in wavelength[58]. Taking into account the energy of the HOMO ($E_F - 2.2$ eV), the higher energy component of S_1 is expected to appear around the low energy cut-off ($E_F + 0 - 0.7$ eV in the intermediate energy ($E_{final} - h\nu$)) and also to exhibit relaxation dynamics on the ps-ns time scale. However, such a spectroscopic feature in the low energy region and the dynamics could not be observed (See Figs 1a and 3a shown below), showing that the formation of lower-lying excitonic states is a minor process in the current $h\nu$ range employed of 4–5 eV. The formation of S_1 and T_1 has been actually reported in 2PPE with different experimental conditions[26,27,30]; a 3 eV pump photon results in a lower efficiency of photocarrier generation than that with $h\nu \sim 4.5$ eV. Furthermore, they employed a higher laser intensity (~sub-μJ/pulse)[26] with low repetition rates (250 kHz) and measured for thicker C_{60} film (20 nm ≈ 25 ML), which may favorably induce excitons by paring the free photocarriers in C_{60} film due to a high photoexcitation density. It should be emphasized again that the enormous intensity around the cut-off with $h\nu > E_{vac}$ in Fig. 1a must be due to direct one photon photoemission from just below E_F.

TR-2PPE results. Figure 3a shows TR-2PPE spectra taken with various pump-probe delays (Δt), where a spectrum at $\Delta t = 9$ ps is subtracted as a background. The LUMO peak survives even at $\Delta t = 3$ ps, while LUMO + 1 decays more quickly within a few hundred fs. The energy positions of these peaks remain almost the same, which again suggests that free electron photocarriers are generated in the early regime. Otherwise, they

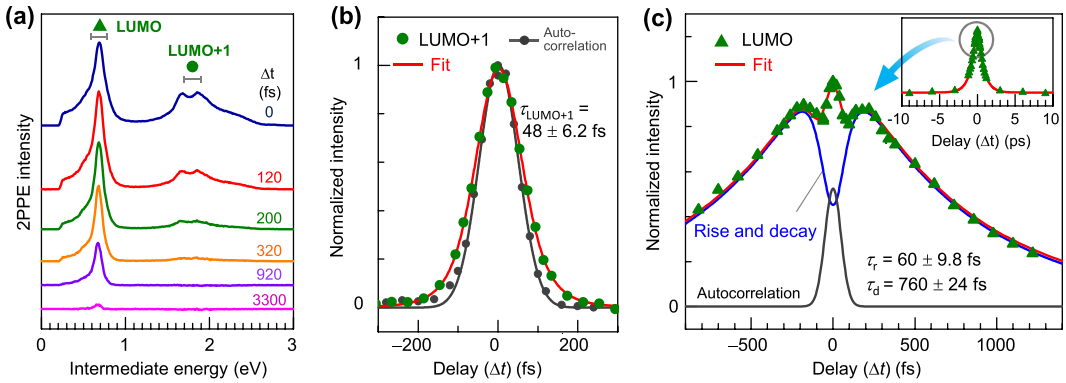

Figure 3. TR-2PPE spectra. (**a**) TR-2PPE spectra ($h\nu = 4.33$ eV) at various Δts. Horizontal axis stands for the intermediate energy defined as $E_{final} - 1\,h\nu$. (**b**) Intensity trace of LUMO + 1 against Δt, where the intensity is obtained from an integration of 0.1 eV width around $E_F + 1.8$ eV marked in **a**. The trace is fitted by a convolution of Gaussian autocorrelation (116 fs in FWHM) and single exponential decay functions. The autocorrelation function was determined in advance from the intensity trace of TR-2PPE for bare HOPG at around $E_F + 1.5$ eV (grey circle). (**c**) Intensity trace for LUMO. Fitted components of the first (Autocorrelation) and second terms (rise and decay) in eq. (1) are also overwritten as solid lines. Inset shows a wider Δt region (±1 ps).

would subsequently form lower-lying excitons, (e.g. S_1 or T_1), which recombine. Figure 3b shows the intensity of LUMO + 1 against Δt. The electron lifetime in the level is 48 ± 6 fs, evaluated by a convolution of a Gaussian autocorrelation (AC) (116 fs in full width at half maximum (FWHM)) and a single exponential decay, where the AC is determined from the intensity trace of the TR-2PPE for bare HOPG at the energy of $E_F + 1.2$–1.7 eV; the lifetime of the electron in the intermediate energy is very short (<20 fs)[59] as compared to the true AC width. As shown in Fig. 3c, interestingly, the signal intensity for LUMO is once again recovered around $\Delta t = 100$–250 fs after the excitation and gradually decreases. Assuming exponential rise and decay processes with time constants of τ_r and τ_d, the time evolution of 2PPE intensity, $I(\Delta t)$, can be described as

$$I(\Delta t) \propto a \int_{-\infty}^{+\infty} \mathrm{AC}(t - \Delta t)(e^{-|t|/\tau_r} - e^{-|t|/\tau_d})dt + b\mathrm{AC}(\Delta t) \quad (1)$$

where a and b are weight factors. In addition to the rise and decay processes of LUMO electrons, the second term of the AC component is taken into account, because photoelectrons at the corresponding energy may include two components of (i) coherent 2PPE from occupied states of HOPG and HOMO − 1 of C_{60} (see Supplementary Fig. S5) and (ii) short-lived hot electrons in the HOPG and C_{60} film, both of which are not regarded as the photocarrier electrons in the LUMO. The TR-2PPE trace for these components should be very similar to the shape of the true AC for the current pulse duration. Eq. (1) reproduces the evolution of the LUMO with $\tau_{r,1ML} = 60 \pm 9.8$ fs and $\tau_{d,1ML} = 760 \pm 24$ fs. Note that the rise time $\tau_{r,1ML}$ is close to the lifetime of LUMO + 1 electron (48 ± 6 fs), suggesting that the LUMO electrons are mainly supplied from highly excited states via LUMO + 1. The LUMO lifetime on HOPG is significantly longer than those for C_{60} on metal substrates[29,43], e.g. Dutton and co-workers have reported that the lifetime increases with the C_{60} thickness on Au(111) from 79 fs at 2 ML to 340 fs at 30 ML, while the corresponding peak has been assigned to a LUMO + 1* exciton[29,43]. Since 2D material substrate of HOPG exhibits weak electronic coupling toward adsorbed species, the decay rate into HOPG is less compared to metal substrates. In fact, the energy positions in the 2PPE spectra for C_{60} films on HOPG show little changes with the C_{60} coverage (Supplementary Figs S1 and S4).

One should also be concerned about the effect of the excitation density on the TR-2PPE results; the recombination of photocarriers generated at different C_{60} molecules (bimolecular recombination) would contribute to the relaxation dynamics. However, the effect is negligible because of the sufficiently low excitation density used in the current study. In the TR-2PPE measurement, assuming a photon flux of ~3×10^{10} photons·cm^{-2} at most (76 MHz, 10 mW, and 0.1 mm spot diameter), three photons are irradiated in an area of 10×10 nm^2 area per pulse (an area consisting of about a hundred of C_{60} molecules). Therefore, the excitation density would be too low to cause bimolecular recombination.

Thickness dependence of LUMO lifetime. Since the sp^2 hybridized nature of the HOPG substrate reduces photocarrier relaxation, the photocarrier hopping rate in a C_{60} film can be evaluated by the C_{60} thickness dependence of the LUMO lifetime. Figure 4a shows the time evolution of LUMO intensities obtained for various coverages of C_{60} films. The recovery of LUMO intensity around $\Delta t = 100$–250 fs becomes unclear at ≥2 ML, while the lifetime of LUMO + 1 is independent of the coverage (see Supplementary Fig. S6). As discussed in the previous section for spectral assignments, 2PPE probes the photocarrier electrons remaining in the topmost C_{60} layer even for the multilayered films. On the other hand, the photocarrier electrons are generated by the pump photon penetrating into whole C_{60} layers. When the photocarrier electrons at the topmost layer initially originate not only from the topmost layer but also at the deeper layers inside, the rise time behavior should become vaguer in the multilayer films, as seen in Fig. 4a. The result therefore indicates that the created photocarriers move around

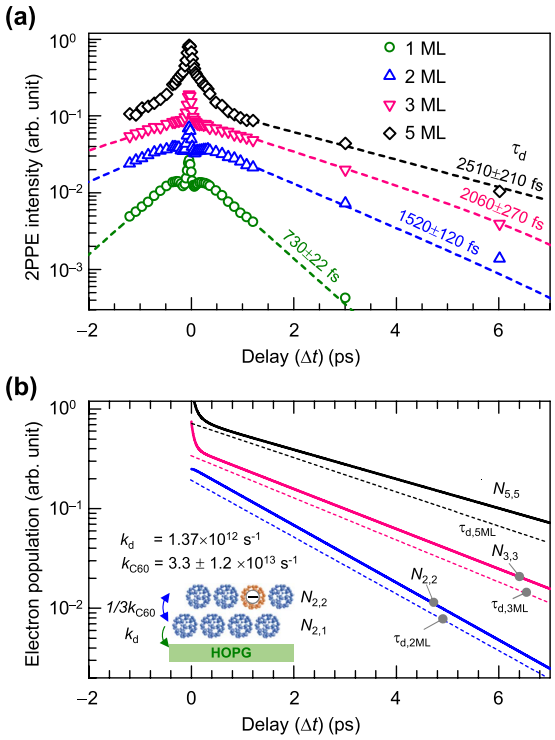

Figure 4. Thickness dependence of LUMO lifetime. (**a**) Intensity of LUMO against Δt for 1, 2, 3, and 5 ML C_{60}. Decay times are fitted using eq. (1) for 1–3 ML, while that for 5 ML is estimated by a slope at $\Delta t > 1$ ps (dotted lines). (**b**) Simulated results with the interlayer hopping model for 2 ML (blue line), 3 ML (pink line), and 5 ML (black line). τ_d obtained in **a** are also shown as exp $(-t/\tau_d)$ (dotted lines) to compare with the simulation (solid lines).

in the C_{60} film with a finite hopping rate. To evaluate the photocarrier hopping rate in the C_{60} film, the thickness dependence of the decay phenomena was modelled for the LUMO electrons.

As shown in Fig. 4a, the LUMO lifetime lengthens with the thickness, and the fitting with eq. (1) shows that τ_d for 1, 2, 3, and 5 ML are 730 ± 22, 1520 ± 120, 2060 ± 270, and 2510 ± 210 fs, respectively. With increases in the C_{60} thickness, a uniform layer-by-layer structure grows without the presence of non-uniform islands (see Supplementary Fig. S7). Since the lifetime of a free electron carrier in solid C_{60} is much longer (ns or μs) than the observed τ_d[60], the decay of photocarriers mainly occurs at the first C_{60} layer interfaced with the substrate. When the photocarrier electron hopping rate from an original C_{60} site to the nearest neighboring C_{60} is defined as k_{C60}, the rate to the specific neighboring C_{60} should be $1/12\, k_{C60}$, because of the fcc crystal structure of a C_{60} film exhibiting a coordination number of twelve. Considering that the fcc's $C_{60}(111)$ surface faces to the vacuum, the interlayer hopping rate from original C_{60} site at the i th layer to the $i+1$ or $i-1$ th layer is $3/12\, k_{C60}$ each (six neighboring C_{60} molecules exist at the i th layer). In addition, it can be assumed that the interlayer hopping from top and bottom layers are modified to be $3/9\, k_{C60}$ owing to the absence of a layer to one side. Based on these concepts, here, the electron population of each layer, $N_{n,m}$, is evaluated, in which n is the total number of C_{60} layers, and m is the targeted C_{60} layer ($1 \le m \le n$). First, we simply evaluate the value of k_{C60} for the result for 2 ML: the number of LUMO electrons at the first interface layer ($N_{2,1}$) and the top layer ($N_{2,2}$) can be simply described by

$$-\frac{dN_{2,1}}{dt} = -\left(\frac{1}{3}k_{C60} + k_d\right)N_{2,1} + \frac{1}{3}k_{C60}N_{2,2} \tag{2}$$

$$-\frac{dN_{2,2}}{dt} = -\frac{1}{3}k_{C60}N_{2,2} + \frac{1}{3}k_{C60}N_{2,1}, \tag{3}$$

where k_d is the decay rate of the photocarrier electron density by relaxing into the substrate from the first C_{60} monolayer, i.e. $k_d = 1/\tau_{d,1ML} = 1.37 \times 10^{12}\ s^{-1}$. Since the irradiated photon penetrates through the C_{60} films, it is reasonable to assume that all of C_{60} layers are uniformly photoexcited as $N_{2,1} = N_{2,2} = 1$ at $t = 0$, whereas the time trace of the TR-2PPE reflects the photocarrier at the top layer ($N_{2,2}$). Then, the above differential equations can be solved numerically for the variable k_{C60}. The blue solid line in Fig. 4b is the simulated result for $N_{2,2}$, where k_{C60} is evaluated to be $3.3 \pm 1.2 \times 10^{13}\ s^{-1}$. So far, the electron hopping rate in unoccupied energy levels has been evaluated by analysis of the resonant autoionization spectrum which has been established as core-hole-clock-spectroscopy[61]. In this method, however, the accessible frequency range of $10^{16} > k > 10^{14}\ s^{-1}$ is limited by the lifetime of the core hole (~a few fs). In fact, Brühwiler *et al.* have evaluated the hopping rate of a LUMO + 1 electron in solid C_{60} to be

$\sim 1.7 \times 10^{14}\,s^{-1}$, while they could not evaluate it for the LUMO[62]. The difference in the hopping rates depending on the energy levels can be explained by the width of the density of states[63]; the hopping rate would become higher for a wider band width. From the resonance window of LUMO + 1 (~0.5 eV) with SAMOs (supplemental material, S3), the band width is larger than that of LUMO (~0.2 eV in FWHM).

The above simulation can also be applied to the result for 3 ML. By using the central value, $3.3 \times 10^{13}\,s^{-1}$, for k_{C60} as obtained above, however, the simulation for 3 ML slightly overestimates the experimental data (not shown). This could be caused by the polarization effect; owing to the reduction of U at the topmost C_{60}, it can be qualitatively deduced that the hopping rate of electrons from an interior C_{60} layer to the topmost layer should be smaller than that from the topmost to an interior layer. Indeed, the result for 3 ML could be well simulated when the former and latter rates are modified to be 2.1×10^{13} and $4.5 \times 10^{13}\,s^{-1}$ (pink solid line in Fig. 4b), respectively, as upper and lower limits of the error for k_{C60} ($\pm 1.2 \times 10^{13}\,s^{-1}$). The reasonable modification falling within its uncertainty suggests the validity of our interlayer hopping model where hopping within an in-plane intralayer does not contribute explicitly. Note that the simulation for 5 ML ($N_{5,5}$) overestimates the experimental result ($\tau_{d,5ML}$), possibly due to thickness inhomogeneity (see Supplementary Fig. S7 for scanning tunneling microscopy images) that could open a decay channel through an edge state of C_{60} layers.

We think that the hopping rate obtained with the above analysis is intrinsic for organic species, but independent of the substrate. The analysis will therefore be also applicable universally for the determination of k_d at the interface between an organic film and a metallic substrate, where k_d is typically too large to be resolved experimentally because of the strong substrate-molecule interaction.

Summary

We observed the hot exciton dissociation and decay dynamics of generated photocarrier electrons in a C_{60} film on a HOPG substrate through the use of TR-2PPE spectroscopy. Unlike metal substrates, the 2D material substrate of HOPG substrate suppresses the electronic interaction with overlayered C_{60} film, which enables us to detect clear time required for photocarrier generation within a hundred fs. The time evolutions of the 2PPE intensity and their C_{60} thickness dependence reveal that the generated photocarriers randomly and frequently hop in the film until decaying into the substrate, where the electron hopping rate in C_{60} is independently and directly evaluated to be $3.3 \pm 1.2 \times 10^{13}\,s^{-1}$. The results have clarified fundamental aspects of photocarrier generation and carrier transportation in organic materials with time-domain measurements, and will provide a key to improving the performance of graphene-based organic devices.

Methods

Sample preparation and 2PPE measurements. Prior to C_{60} deposition, an HOPG substrate was cleaved in air and cleaned by heating (670 K, 50 h) in an ultrahigh vacuum (UHV) chamber, where the base pressure was better than 1×10^{-8} Pa. C_{60} was then deposited in the UHV system with a rate of 0.07 ML/min, monitoring with a quartz microbalance. The C_{60} coverage was calibrated from 2PPE measurements (Supplementary Figs S1 and S2). TR-2PPE measurements were carried out using the third harmonics ($h\nu = 4.13$–4.77 eV, p-polarization) of a Ti:sapphire laser (~100 fs, 76 MHz), which was separated into pump and probe photons with a beam splitter. Both pump and probe photons are recombined at the sample in UHV with a concave mirror ($f = 400$ mm). In this optical configuration ("skew configuration") the autocorrelation of incident photons can approximate a Gaussian peak function without interference oscilation[31]. Photoelectrons emitted in the normal direction were detected by a hemispherical electron energy analyzer (VGSCIENTA: R3000), where the energy of photoelectron was calibrated by UPS of an Au plate providing a clear Fermi edge as zero binding energy at $E_{final} = E_F + h\nu$ (21.22 eV) for E_{final} (Supplementary Fig. S5). A sample bias of −3 V was applied to collect low-energy photoelectrons around the cut-off energy (E_{vac}). Energy and time resolutions of the TR-2PPE system were about 20 meV and 20 fs, respectively. The sample temperature was 293 K during the TR-2PPE measurement.

References

1. Geim, A. K. & Novoselov, K. S. The rise of graphene. *Nature Mater*. **6,** 183–191 (2007).
2. Castro Neto, A. H., Guinea, F., Peres, N. M. R., Novoselov, K. S. & Geim, A. K. The electronic properties of graphene. *Rev. Mod. Phys*. **81,** 109–162 (2009).
3. Wu, J. *et al.* Organic solar cells with solution-processed graphene transparent electrodes. *Appl. Phys. Lett*. **92,** 263302 (2008).
4. Wang, Q. H. & Hersam, M. C. Room-temperature molecular resolution characterization of self-assembled organic monolayers on epitaxial graphene. *Nature Chem*. **1,** 206–211 (2009).
5. Mao, J. H. *et al.* Tunability of Supramolecular Kagome Lattices of Magnetic Phthalocyanines Using Graphene-Based Moiré Patterns as Templates. *J. Am. Chem. Soc*. **131,** 14136–14137 (2009).
6. Dichtel, W. R. *et al.* J. Oriented 2D Covalent Organic Framework Thin Films on Single-Layer Graphene. *Science* **332,** 228–231 (2011).
7. Yu, D., Park, K., Durstock, M. & Dai, L. J. Fullerene-Grafted Graphene for Efficient Bulk Heterojunction Polymer Photovoltaic Devices. *J. Phys. Chem. Lett*. **2,** 1113–1118 (2011).
8. Cho, J. *et al.* Structural and Electronic Decoupling of C_{60} from Epitaxial Graphene on SiC. *Nano Lett*. **12,** 3018–3024 (2012).
9. Lu, J. *et al.* Using the Graphene Moiré Pattern for the Trapping of C_{60} and Homoepitaxy of Graphene. *ACS Nano* **6,** 944–950 (2012).
10. Salzmann, I. *et al.* Epitaxial Growth of π-Stacked Perfluoropentacene on Graphene-Coated Quartz. *ACS Nano*. **6,** 10874–10883 (2012).
11. Schlierf, A., Samorì, P. & Palermo, V. Graphene-organic composites for electronics: Optical and electronic interactions in vacuum, liquids and thin solid films. *J. Mater. Chem. C*. **2,** 3129–3143 (2014).
12. Yin, Z. *et al.* Graphene-Based Materials for Solar Cell Applications. *Adv. Energy Mater.* **1,** 1–19 (2014).
13. Christodoulou, C. *et al.* Tuning the Electronic Structure of Graphene by Molecular Dopants: Impact of the Substrate. *ACS Appl. Mater. Interfaces* **7,** 19134–19144 (2015).
14. Kim, K. *et al.* Structural and Electrical Investigation of C_{60} Graphene Vertical Heterostructures. *ACS Nano* **9,** 5922–5928 (2015).
15. Kroto, H. W., Heath, J. R., O'Brien, S. C., Curl, R. F. & Smalley R. E. C_{60}: Buckminsterfullerene. *Nature* **318,** 162–163 (1985).
16. Yu, G., Gao, J., Hummelen, J. C., Wudl, F. & Heeger, A. J. Polymer photovoltaic cells: enhanced efficiencies via a network of internal donor-acceptor heterojunctions. *Science* **270,** 1789–1791 (1995).
17. Yoo, S., Domercq, B. & Kippelen, B. Efficient thin-film organic solar cells based on pentacene/C_{60} heterojunctions. *Appl. Phys. Lett*. **85,** 5427–5429 (2004).

18. Kim, Y. *et al.* A strong regioregularity effect in self-organizing conjugated polymer films and high-efficiency polythiophene:fullerene solar cells. *Nature Mater*. **5,** 197–203 (2006).
19. Kandada, A. R. S. *et al.* Ultrafast Energy Transfer in Ultrathin Organic Donor/Acceptor Blend. *Sci. Rep*. **3,** 2073, 10.1038/srep02073 (2013).
20. Grancini, G. *et al.* Hot exciton dissociation in polymer solar cells. *Nat. Mater.* **12,** 29–33 (2013).
21. Lane, P. A., Cunningham, P. D., Melinger, J. S., Esenturk, O. & Heilweil, E. J. Hot photocarrier dynamics in organic solar cells. *Nature Commun*. **6,** 7558, 10.1038/ncomms8558 (2015).
22. Lof, R. W., van Veenendaal, M. A., Koopmans, B., Jonkman, H. T. & Sawatzky, G. A. Band gap, excitons, and Coulomb interaction in solid C_{60}, *Phys. Rev. Lett*. **68,** 3924–3927 (1992).
23. Kazaoui, S., Ross, R. & Minami, N. Intermolecular charge-transfer excitation in C_{60} films: Evidence from luminescence and photoconductivity. *Phys. Rev. B* **52,** R11665–R11667 (1995).
24. Dick, D. *et al.* Transient spectroscopy of excitons and polarons in C_{60} films from femtoseconds to milliseconds. *Phys. Rev. Lett.* **73,** 2760–2763 (1994).
25. Fleischer, S. B. *et al.* Phototransformation in visible and near-IR femtosecond pump-probe studies of C_{60} films. *Appl. Phys. Lett*. **69,** 296–298 (1996).
26. Jacquemin, R., Kraus, S. & Eberhardt, W. Direct observation of the dynamics of excited electronic states in solids: F-Sec time resolved photoemission of C_{60}. *Solid State Commun*. **105,** 449–453 (1998).
27. Link, S., Scholl, A., Jacquemin, R. & Eberhardt, W. Electron dynamics at a Ag/C_{60} metal–semiconductor interface. *Solid State Commun*. **113,** 689–693 (2000).
28. Dutton, G. & Zhu, X.-Y. Unoccupied States in C_{60} Thin Films Probed by Two-Photon Photoemission. *J. Phys. Chem. B* **106,** 5975–5981 (2002).
29. Dutton, G. Quinn, D. P., Lindstrom, C. D. & Zhu, X.-Y. Exciton dynamics at molecule-metal interface: C_{60}/Au(111). *Phys. Rev. B* **72,** 045441 (2005).
30. Rosenfeldt, A. C., Göhler, B. & Zacharias, H. Time-resolved photoelectron spectroscopy of low-energy excitations of 4×4 C_{60}/Cu(111). *J. Chem. Phys*. **133,** 234704 (2010).
31. Petek, H. & Ogawa, S. Femtosecond time-resolved two-photon photoemission studies of electron dynamics in metals. *Prog. Surf. Sci.* **56,** 239–310 (1997).
32. Echenique, P. M. *et al.* Decay of electronic excitations at metal surfaces. *Surf. Sci. Rep*. **52,** 219–317 (2004).
33. Armbrust, N., Güdde, J., Jakob, P. & Höfer, U. Time-Resolved Two-Photon Photoemission of Unoccupied Electronic States of Periodically Rippled Graphene on Ru(0001). *Phys. Rev. Lett.* **108,** 056801 (2012).
34. Niesner, N. *et al.* Trapping Surface Electrons on Graphene Layers and Islands. *Phys. Rev. B* **85,** 081402(R) (2012).
35. Giesen, K., Hage, F., Himpsel, F. J., Riess, H. J. & Steinmann, W. Two-photon photoemission via image-potential states. *Phys. Rev. Lett*. **55,** 300–303 (1985).
36. Feng, M., Zhao, J. & Petek, H. Atomlike, Hollow-Core-Bound Molecular Orbitals of C_{60}. *Science* **320,** 359–362 (2008).
37. Zhao, J., Feng, M. & Petek, H. The Superatom States of Fullerenes and Their Hybridization into the Nearly Free Electron Bands of Fullerites. *ACS Nano* **3,** 853–864 (2009).
38. Dutton, G. J., Dougherty, D. B., Jin, W., Reutt-Robey, J. E. & Robey, S. W. Superatom orbitals of C_{60} on Ag(111): Two-photon photoemission and scanning tunneling spectroscopy. *Phys. Rev. B* **84,** 195435 (2011).
39. Chan, W.-L. *et al.* Communication: Momentum-resolved quantum interference in optically excited surface states. *J. Chem. Phys*. **135,** 031101 (2011).
40. Feng, M., Zhao, J., Huang, T., Zhu, X.-Y. & Petek, H. The Electronic Properties of Superatom States of Hollow Molecules. *Acc. Chem. Res*. **44,** 360–368 (2011).
41. Mignolet, B., Johansson, J. O., Campbell, E. E. B. & Remacle, F. Probing rapidly-ionizing super-atom molecular orbitals in C_{60}: A computational and femtosecond photoelectron spectroscopy study. *ChemPhysChem* **14,** 3332–3340 (2013).
42. Rudolf, P., Golden, M. S. & Brühwiler, P. A. Studies of fullerenes by the excitation, emission, and scattering of electrons. *J. Elect. Spectrosc. Relat. Phenom*. **100,** 409–433 (1999).
43. Dutton, G. & Zhu, X.-Y. Distance-Dependent Electronic Coupling at Molecule-Metal Interfaces: C_{60}/Cu(111). *J. Phys. Chem. B* **108,** 7788–7793 (2004).
44. Dresselhaus, M. S., Dresselhaus, G. & Eklund, P. C. *Science of Fullerenes and Carbon Nanotubes*. (Academic Press, 1996).
45. Kremer, R. K. *et al.* High-temperature conductivity study on single-crystal C_{60}. *Appl. Phys. A* **56,** 211–214 (1993).
46. Beu, T. A., Onoe, J. & Hida, A. First-principles calculations of the electronic structure of one-dimensional C_{60} polymers. *Phys. Rev. B* **72,** 155416 (2005).
47. Pudlak, M. & Pincak, R. Energy gap between highest occupied molecular orbital and lowest unoccupied molecular orbital in multiwalled fullerenes. *Phys. Rev. A* **79,** 033202 (2009).
48. Zhao, W. & Kahn, A. Charge transfer at n-doped organic-organic heterojunctions. *J. Appl. Phys*. **105,** 123711 (2009).
49. Brühwiler, P. A., Maxwell, A. J., Nilsson, A., Mårtensson, N. & Gunnarsson, O. Auger and photoelectron study of the Hubbard *U* in C_{60}, K_3C_{60}, and K_6C_{60}. *Phys. Rev. B* **48,** 18296–18299 (1993).
50. Tzeng, C. T., Tsuei, K. D., Cheng, H. M. & Chu, R. Y. Covalent bonding and hole–electron Coulomb interaction *U* in C_{60} on Be(0001) surfaces. *J. Phys.: Condens. Matter* **19,** 176009, 10.1088/0953-8984/19/17/176009 (2007).
51. Torrente, I. F., Franke, K. J. & Pascual, J. I. Spectroscopy of C_{60} single molecules: the role of screening on energy level alignment. *J. Phys.: Condens. Matter* **20,** 184001, 10.1088/0953–8984/20/18/184001 (2008).
52. Tahara, T. *Advances in Multi-Photon Processes and Spectroscopy*, Vol. 16, Chap. 1 (ed. Lin, S. H., Villaeys, A. A. & Fujimura, Y.) (World Scientific Publishing Company, 2004).
53. Varene, E., Bogner, L., Bronner, C. & Tegeder, P. Ultrafast Exciton Population, Relaxation, and Decay Dynamics in Thin Oligothiophene Films. *Phys. Rev. Lett*. **109,** 207601 (2012).
54. Shibuta, M., Hirata, N., Eguchi, T. & Nakajima, A. Probing of an Adsorbate-Specific Excited State on an Organic Insulating Surface by Two-Photon Photoemission Spectroscopy. *J. Am. Chem. Soc.* **136,** 1825–1831 (2014).
55. Cheville, R. A. & Halas, N. J. Time-resolved carrier relaxation in solid C_{60} thin films. *Phys. Rev. B* **45,** 4548–4550 (1992).
56. Bauernschmitt, R., Ahlrichs, R., Hennrich, F. H. & Kappes, M. M. Experiment Values Time Dependent Density Functional Theory Prediction of Fullerene Electronic Absorption. *J. Am. Chem. Soc.* **120,** 5052–5059 (1998).
57. Shirley, E. L., Benedict, L. X. & Louie, S. G. Excitons in Solid C_{60}. *Phys. Rev. B* **54,** 10970–10977 (1996).
58. Pavlovich, V. S. & Shpilevsky, E. M. Absorption and fluorescence spectra of C_{60} fullerene concentrated solutions in hexane and polystyrene at 77–300 K. *J. Appl. Spec*. **77,** 362–369 (2010).
59. Moos, G., Gahl, C., Fasel, R., Wolf, M. & Hertel, T. Anisotropy of Quasiparticle Lifetimes and the Role of Disorder in Graphite from Ultrafast Time-Resolved Photoemission Spectroscopy. *Phys. Rev. Lett*. **87,** 267402 (2001).
60. Lee, C. H., Yu, G., Kraabel, B., Moses, D. & Srdanov, V. I. Effects of oxygen on the photocarrier dynamics in a C_{60} film: Studies of transient and steady-state photoconductivity. *Phys. Rev. B* **49,** 10572–10576 (1994).
61. Föhlisch, A. *et al.* Direct observation of electron dynamics in the attosecond domain. *Nature* **436,** 373–376 (2005).
62. Brühwiler, P. A. *et al.* C 1*s* autoionization study of electron hopping rates in solid C_{60}. *Phys. Rev. Lett*. **71,** 3721–3724 (1993).
63. Brédas, J. L., Calbert, J. P., da Silva Filho, D. A. & Cornil, J. Organic semiconductors: A theoretical characterization of the basic parameters governing charge transport. *Proc. Natl. Acad. Sci. USA* **99,** 5804–5809 (2002).

Acknowledgements
This work is partly supported by the Science Research Promotion Fund from the Promotion and Mutual Aid Corporation for Private Schools of Japan, and by JSPS KAKENHI of Grant-in-Aids for Young Scientists (B) Grant Number 25810010 and for Scientific Research (A) Grant Number 15H02002.

Author Contributions
M.S., K.Y. and T.O. performed the TR-2PPE experiments and data analysis. M.N. and T.E. took the STM images of C_{60} film on graphite. M.S., T.E. and A.N. wrote the manuscripts. A.N. supervised the research project.

Additional Information
Supplementary information accompanies this paper at http://www.nature.com/srep

Competing financial interests: The authors declare no competing financial interests.

How to cite this article: Shibuta, M. *et al.* Direct observation of photocarrier electron dynamics in C_{60} films on graphite by time-resolved two-photon photoemission. *Sci. Rep.* **6**, 35853; doi: 10.1038/srep35853 (2016).